Routes to Carboxylic Acid Functional Acrylonitrile Copolymers via *N-tert*-Butyl-*N*-(1-diethylphosphono-2,2-dimethylpropyl) Free Nitroxide Based Nitroxide-Mediated Polymerization

Valerie Consolante,[1] Milan Maric,[1] Alexander Penlidis[2]

[1]*Department of Chemical Engineering, McGill University, McGill Institute of Advanced Materials (MIAM), Centre for Self-Assembled Chemical Structures (CSACS), 3610 University Street, Montreal, Quebec H3A 2B2, Canada*
[2]*Department of Chemical Engineering, Institute for Polymer Research, University of Waterloo, Waterloo, Ontario N2L 3G1, Canada*

Received 22 July 2011; accepted 24 November 2011
DOI 10.1002/app.36547
Published online in Wiley Online Library (wileyonlinelibrary.com).

ABSTRACT: Styrene (S)/acrylonitrile [AN; initial acrylonitrile molar feed compositions ($f_{AN,0}$'s) = 0.10–0.86) and *tert*-butyl methacrylate (*t*BMA)/AN ($f_{AN,0}$ = 0.10–0.80) copolymers were synthesized at 90°C in 50 wt % 1,4-dioxane solutions with a unimolecular initiator, *N*-(2-methylpropyl)-*N*-(1-diethylphosphono-2,2-dimethylpropyl)-*O*-(2-carboxylprop-2-yl) hydroxylamine [BlocBuilder (BB)]. In the *t*BMA/AN copolymerizations, 8.0–8.5 mol % *N-tert*-butyl-*N*-(1-diethylphosphono-2,2-dimethylpropyl) free nitroxide relative to BB was added. The S/AN copolymers exhibited narrow, monomodal molecular weight distributions (MWDs) with low polydispersities [weight-average molecular weight (M_w)/number-average molecular weight (M_n) = 1.14–1.26], and the M_n versus monomer conversion (X) plots were relatively linear (M_n = 18.1 kg/mol, $X \approx 0.7$); this suggested that pseudo-living behavior was approached. AN proved to be an effective controlling comonomer for *t*BMA because the *t*BMA/AN copolymers exhibited narrow monomodal MWDs with M_w/M_n = 1.17–1.50 and relatively linear M_n versus X plots to reasonably high X values (M_n = 15.6 kg/mol, $X \approx 0.6$). The AN and S monomer reactivity ratios were $r_{AN} = 0.07 \pm 0.01$ and $r_S = 0.27 \pm 0.02$ (Fineman–Ross) and $r_{AN} = 0.10 \pm 0.01$ and $r_S = 0.28 \pm 0.02$ (Kelen–Tüdos), respectively; these values were in good agreement with conventional free-radical polymerization. Error-in-variables model (EVM) analysis indicated that the use of cumulative composition S/AN data was more effective than typical approaches using low-X data with the Mayo–Lewis model. The AN and *t*BMA reactivity ratios [$r_{AN} = 0.07 \pm 0.01$ and $r_{tBMA} = 1.24 \pm 0.20$ (Fineman–Ross) and $r_{AN} = 0.14 \pm 0.01$ and $r_{tBMA} = 0.89 \pm 0.19$ (Kelen–Tüdos)] were similar to those reported for related alkyl methacrylate/AN conventional radical copolymerizations. EVM analysis suggested significant experimental error was associated with the *t*BMA/AN system, and this warrants further investigation. © 2012 Wiley Periodicals, Inc. J Appl Polym Sci 000: 000–000, 2012

Key words: copolymerization; polystyrene; radical polymerization

INTRODUCTION

Products such as gasoline and other pure or mixed hydrocarbon solvents, as well as gas molecules, can easily permeate polyethylene (PE) containers.[1] To overcome these permeability problems, appropriate polymer blending into PE is done to develop two-phase morphologies that act as barriers.[1–3] Many examples exist in the literature, such as the blending of nylon into a polyolefin that has been suitably functionalized so that the morphology is stabilized by an *in situ* reaction during the melt blending between appropriate functional groups between the nylon and the polyolefin.[2–10] This approach is limited to commercially available polymers with inherent functionality from the polymerization process (nylon has terminal primary amine groups). To produce a more versatile range of barrier materials, it is desirable to include polymers where the functional group is not a direct residue of the original polymerization process, such as nylon. It may also be beneficial to place a single functional group at the chain end or to restrict the functional groups to one part of the chain because the placement of functional groups has a dramatic effect on the reactivity and, thus, on the blend morphology.[11]

We aimed to develop barrier polymers based on poly(styrene-*ran*-acrylonitrile) copolymers [poly(S/AN)s] that had functional groups either on the chain

Correspondence to: M. Maric (milan.maric@mcgill.ca).
Contract grant sponsor: Canadian Foundation for Innovation New Opportunities Fund (Imperial Oil University Research Award).

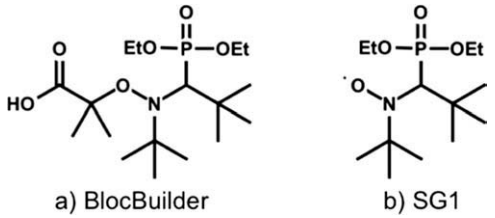

Scheme 1 Structures of (a) BB and (b) SG1.

end or along the chain. Styrene (S)/acrylonitrile (AN)-type copolymers have long been used because of their excellent grease resistance and oxygen and carbon dioxide barrier properties at higher AN loadings.[12] AN-based copolymers can have their microstructure easily controlled by controlled radical polymerization (CRP), which approaches the narrow molecular weight distribution (MWD) and the ability to control microstructure comparable to that of living or ionic polymerizations without the need for air-free transfers, careful purification of reagents, or functional-group protection typically required of the latter.[13]

Nitroxide-mediated polymerization (NMP) is desirable because of its simplicity, particularly when one uses unimolecular initiators, such as *N*-(2-methylpropyl)-*N*-(1-diethylphosphono-2,2-dimethylpropyl)-*O*-(2-carboxylprop-2-yl) hydroxylamine [BlocBuilder (BB); commercially available from Arkema, Inc., King of Prussia, PA, Scheme 1].[14] There is significant literature concerning S/AN copolymerizations by CRP methods, including reversible addition–fragmentation chain-transfer polymerization,[15,16] atom-transfer radical polymerization,[17–19] and NMP.[20–26] Most studies have focused on S/AN feed compositions near the azeotropic composition ($\sim$ 60 mol % S), although several researchers have examined AN homopolymerization,[27–31] particularly and most recently using cobalt-mediated radical polymerization.[32,33] S/AN has not been specifically copolymerized with BB. This is relevant because BB provides sufficient control of polymerization but with much faster polymerization rates compared to first-generation nitroxides, such as 2,2-tetramethyl piperidine (TEMPO). Furthermore, BB has been able to control a wider range of monomers previously unattainable by TEMPO and be effective at much lower temperatures. The study of BB-mediated S/AN compositions is of interest because commercially important S/AN copolymers can be accessed and combined with other monomers to form copolymers with a much wider range of properties. Furthermore, AN, like S, is a suitable controlling comonomer for methacrylate polymerizations via BB.[34] Thus, AN not only serves to impart favorable barrier properties but also enables the BB-controlled polymerization of methacrylic monomers.

We focused initially on carboxylic acid (COOH)-functional S/AN because many commercially PE resins are available with grafted epoxy functional glycidyl methacrylate and permit blend stabilization with a carboxylic acid/epoxy reaction.[6] Such groups have been used in commercial blend systems[35] and can also be readily introduced into resins with CRP.[36] In particular, S/AN resins made from BB would be well suited as they would have a carboxylic acid at the chain end from the initiator residue. Furthermore, if desired, additional carboxylic acid groups could be introduced along the chain or in one block by the incorporation of a carboxylic acid containing monomer, such as acrylic or methacrylic acid (and their protected forms, e.g., *tert*-butyl acrylate or methacrylate).

Thus, we examined two families of resins with the goal of introducing carboxylic acids at the chain end or at random places along the chain into S/AN resins (Scheme 2). The placement of the carboxylic acid groups on the chain end was done by S/AN copolymerizations with BB. A wide range of S/AN compositions were, thus, studied to determine how much AN could be incorporated into the final copolymer. Random placement of the carboxylic acid was initially examined first by the copolymerization of *tert*-butyl methacrylate (*t*BMA) with AN. *t*BMA was chosen for a couple of reasons: (1) it would not degrade the *N*-*tert*-butyl-*N*-(1-diethylphosphono-2,2-dimethylpropyl) free nitroxide (SG1) as the acidic form of the monomer would, and (2) the methacrylate is not susceptible to the back-biting chain-transfer reactions to which the acrylate is prone.[37] Furthermore, we aimed to determine whether AN was also an effective controller for *t*BMA over a wider range of AN feed compositions as it has been for methyl methacrylate (MMA).[34] By studying these two binary copolymerizations, we were able to develop initial designs for AN-based barrier polymers for suitable reactive blending with PE matrices.

EXPERIMENTAL

Materials

AN (99%), S (99%), and *t*BMA (98%) were purchased from Sigma-Aldrich, Oakville, ON, Canada and were purified by passage through a column of basic alumina (Brockmann, type 1, 150 mesh) mixed with 5% calcium hydride (90–95%, reagent grade), then sealed with a head of nitrogen, and stored in a refrigerator until it was needed. Hexane (98.5%), methanol (99.8%), tetrahydrofuran (THF; 99.9%), dimethylformamide (DMF; High Pressure Liquid Chromatography (HPLC) grade, 99.9%), and 1,4-dioxane (99.8%) were obtained from Fisher Canada (Whitby, ON, Canada) and were used as received. *N*-(2-Methylpropyl)-*N*-(1-diethylphosphono-2,2-dimethylpropyl)-*O*-(2-carboxylprop-2-yl) hydroxylamine

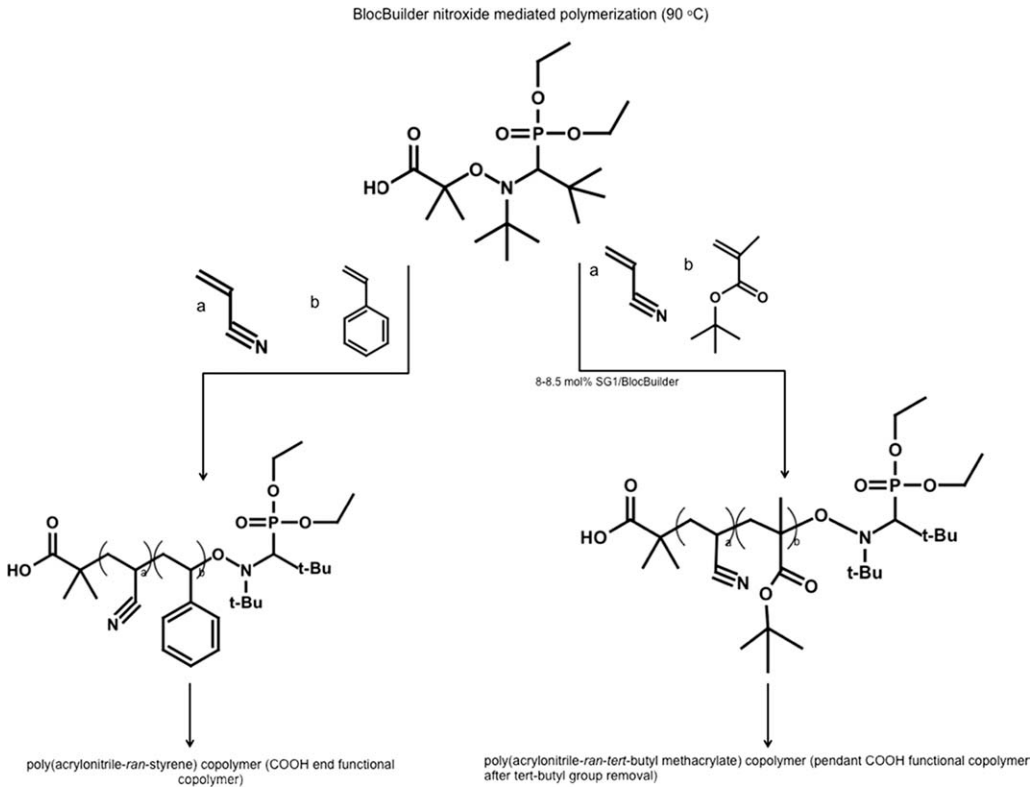

Scheme 2 Routes for carboxylic acid functional AN copolymers with the S/AN copolymerization with BB to give the acid-terminal copolymer, whereas *t*BMA/AN copolymerizations with BB yielded pendant-functional copolymers after cleavage of the *tert*-butyl groups.

(BB; 99%) was obtained from Arkema, and SG1 (85%) was kindly donated by Noah Macy of Arkema and was used as received. Polystyrene (PS; $M_n = 13.0$ kg/mol, $M_w/M_n = 1.10$), polyacrylonitrile (PAN; $M_n = 60.6$ kg/mol, $M_w/M_n = 1.70$), and poly(*tert*-butyl methacrylate) (P*t*BMA; $M_n = 38.5$ kg/mol, $M_w/M_n = 1.01$) were used as standards for Fourier transform infrared (FTIR) spectroscopy and were obtained from Scientific Polymer Products, Inc., Ontario, NY.

Synthesis of poly(S/AN)

Several nitroxide-mediated copolymerization experiments of S and AN in 1,4-dioxane were conducted at 90°C with only BB as the nitroxide. All copolymerizations were performed in a 50-mL, three-necked round-bottom glass flask equipped with a magnetic stirring bar, condenser, and thermal well. The flask was set inside a heating mantle and placed on a magnetic stirrer. Formulations for initial AN molar feed compositions ($f_{AN,0}$'s) of 0.10–0.70 were followed and are found in Table I. All of the polymerizations were conducted in 50 wt % 1,4-dioxane solutions (50 wt % of monomer in solvent). The target molecular weight at complete conversion ($M_{n,target}$) at complete X, calculated by the mass of the monomer relative to the moles of BB initiator, was set to approximately 25 kg/mol in all cases. The initiator, solvent, and monomer were added to the flask with the stirrer. As an example, for the synthesis of S/AN–BB-30 (where the number after the hyphen indicates the BB molar feed composition with respect to AN), BB (0.102 g, 0.267 mmol) and the stirrer were added to the flask, which was then sealed with a rubber septum. S (5.60 g, 0.0538 mol), AN (1.22 g, 0.0230 mol), and 1,4-dioxane (6.80 g, 0.0772 mol) were each injected into the flask. The central neck was connected to a condenser and capped with a rubber septum with a needle to relieve pressure applied by the nitrogen purge throughout the reaction. A thermocouple was connected to a controller and inserted into the third neck of the flask. As stirring began and the

TABLE I
S/AN Copolymerization Formulations for Various Compositions with BB at 90°C in 1,4-Dioxane

Experiment ID[a]	$f_{AN,0}$	$[BB]_0$ (M)	$[S]_0$ (M)	$[AN]_0$ (M)	$[Dioxane]_0$ (M)
S/AN–BB-10	0.10	0.019	4.38	0.48	5.46
S/AN–BB-30	0.30	0.019	3.77	1.61	5.41
S/AN–BB-40	0.40	0.019	3.46	2.29	5.30
S/AN–BB-50	0.50	0.019	3.01	3.10	5.29
S/AN–BB-70	0.70	0.018	2.07	4.72	5.30

[a] All S/AN copolymerizations were done in 50 wt % 1,4-dioxane at 90°C.

TABLE II
***t*BMA/AN Copolymerization Formulations for Various Compositions with BB/SG1 at 90°C in 1,4-Dioxane**

Experiment ID[a]	$f_{AN,0}$	$[BB]_0$ (*M*)	$[SG1]_0$ (*M*)	r[b]	$[tBMA]_0$ (*M*)	$[AN]_0$ (*M*)	$[Dioxane]_0$ (*M*)
*t*BMA/AN–BB/SG1-11	0.11	0.021	0.002	0.081	3.54	0.44	4.92
*t*BMA/AN–BB/SG1-30	0.30	0.019	0.002	0.080	2.86	1.21	5.30
*t*BMA/AN–BB/SG1-51	0.51	0.019	0.002	0.085	2.47	2.57	4.98
*t*BMA/AN–BB/SG1-70	0.70	0.019	0.002	0.081	1.80	4.17	5.06
*t*BMA/AN–BB/SG1-80	0.80	0.019	0.002	0.080	1.34	5.46	5.01

[a] All of the *t*BMA/AN copolymerizations were done in 50 wt % 1,4-dioxane at 90°C. *t*BMA/AN–BB/SG1-*xx* refers to *t*BMA/AN copolymerizations done with BB/SG1 and *xx* refers to the molar feed composition with respect to AN.
[b] r, initial molar ratio of SG1 to BB ($[SG1]_0/[BB]_0$).

monomers were well mixed, the chilling unit (Neslab 740, Thermo Fisher Scientific, Asheville, NC) using a glycol/water mixture that was connected to the condenser was set to 5°C. A nitrogen flow was introduced to purge the solution for 30 min. The reactor was heated to 90°C at a rate of about 5°C/min, with the purge maintained. Once the reaction reached the set-point temperature, the first sample was taken [time (t) = 0, start of the reaction] with a 1-mL syringe followed by periodic sampling until the solution became too viscous for the withdrawal of any more samples. The samples were precipitated in hexane, left to settle for several hours, and then decanted and dried overnight in a vacuum oven at 60°C. For a particular example, the final yield of S/AN–BB-30 after 240 min was 3.41 g (50% X on the basis of gravimetry) with M_n = 16.6 kg/mol and M_w/M_n = 1.17, as determined by gel permeation chromatography (GPC) calibrated relative to linear poly(methyl methacrylate) (PMMA) standards in DMF at 50°C and corrected with composition-averaged Mark–Houwink parameters (see the Characterization section for full details).

Synthesis of *tert*-butyl methacrylate/acrylonitrile random copolymers [poly(tBMA-*ran*-AN)s]

Nitroxide-mediated copolymerizations of *t*BMA and AN in 50 wt % 1,4-dioxane solution were conducted at 90°C with BB and additional SG1. All of the copolymerizations were performed similarly to the S/AN copolymerizations. A 50-mL, three-necked, round-bottom glass flask equipped with a magnetic stirring bar, condenser, and thermal well was used. The flask was set inside a heating mantle and placed on a magnetic stirrer. Formulations for $f_{AN,0}$'s from 0.10–0.80 were followed and are found in Table II. $M_{n,target}$, calculated on the basis of the masses of the *t*BMA and AN monomers relative to BB, were nearly 25 kg/mol for each of the experiments. For the *t*BMA/AN copolymerizations, 8.1–8.5 mol % SG1 relative to BB was used to provide additional control of the polymerization. The initiator, solvent, and monomer were added to the flask with the stirrer. For example, for experiment ID *t*BMA/AN–BB-30, BB (0.0975 g, 0.256 mmol) and SG1 (0.008 g, 0.02 mmol) were added to the flask, which was then sealed with a rubber septum. *t*BMA (5.58 g, 0.0392 mol), AN (0.908 g, 0.0171 mol), and 1,4-dioxane (6.40 g, 0.0726 mol) were each injected into the flask with disposable 5-mL syringes to accurately obtain the required feed compositions. The central neck was connected to a condenser and capped with a rubber septum with a needle to relieve pressure applied by the nitrogen purge throughout the reaction. A thermocouple was connected to a controller and inserted into the third neck of the flask. As stirring began and the monomers were mixed, the chilling unit (Neslab 740) using a glycol/water mixture that was connected to the condenser was set to 5°C. A nitrogen flow was introduced to purge the solution for 30 min. The reactor was heated to 90°C at a rate of about 5°C/min with the purge maintained. Once the reaction reached the set-point temperature, the first sample was taken (t = 0, start of the reaction) with a 1-mL syringe followed by periodic sampling until the solution became too viscous for the withdrawal of more samples. The samples were precipitated in a 70% w/w methanol/distilled water mixture, left to settle for several hours, and then decanted and dried overnight in a vacuum oven at 60°C. In particular, for the synthesis of *t*BMA/AN–BB-30, the final yield after 350 min was 3.61 g (55% X on the basis of gravimetry) with M_n = 10.4 kg/mol and M_w/M_n = 1.35, as determined by GPC calibrated with linear PS standards in THF at 40°C and corrected with composition-averaged Mark–Houwink parameters (see the Characterization section for full details).

Characterization

The molecular weight and MWD of the copolymers were characterized by GPC with a Waters Breeze (Milford, MA) system equipped with three Styragel columns (molecular weight ranges of the columns: HR1 = 10^2 to 5×10^3 g/mol, HR2 = 5×10^2 to 2×10^4 g/mol, and HR3 = 5×10^3 to 6×10^5 g/mol) and a guard column heated to 50°C during analysis. DMF was used as the mobile phase for the S/AN copolymers because the copolymers were not all fully

soluble in THF. THF was used as the mobile phase for the *t*BMA/AN copolymers because the copolymers were all soluble in THF. The eluent flow rate was 0.3 mL/min during analysis. The GPC instrument was also equipped with ultraviolet (UV 2487) and differential refractive index (RI 2410) detectors. The molecular weights were calibrated relative to linear, narrow-MWD PS standards (when we used THF) and PMMA standards (when we used DMF). The copolymer molecular weights were corrected with the Mark–Houwink relationship (intrinsic viscosity $[\eta] = KM^{\alpha}$, where K and α are the Mark-Houwink parameters and M is the molecular weight) on the basis of the following coefficients: $K_{PS} = 11.4 \times 10^{-5}$ dL/g and $\alpha_{PS} = 0.716$ in THF at 40°C,[38] $K_{PtBMA} = 11.2 \times 10^{-5}$ dL/g and $\alpha_{PtBMA} = 0.692$ in THF at 30°C,[39] $K_{PAN} = 21.2 \times 10^{-5}$ dL/g and $\alpha_{PAN} = 0.75$ in DMF at 60°C (data at 50°C was not available).[40] The S/AN copolymers in DMF at various AN compositions in the copolymer (F_{AN}'s) were also used to estimate the S/AN copolymer molecular weights: $K_{S/AN} = 1.62 \times 10^{-4}$ dL/g and $\alpha_{S/AN} = 0.75$ ($F_{AN} = 0.40$, $T = 30$°C)[41] and $K_{S/AN} = 1.2 \times 10^{-4}$ dL/g, and $\alpha_{S/AN} = 0.77$ ($F_{AN} = 0.626$, T = 30°C).[42] For the PMMA standards used in DMF, $K_{PMMA} = 2.07 \times 10^{-5}$ dL/g and $\alpha_{PMMA} = 0.632$ in DMF at 50°C.[43] The molecular weights were corrected by compositional averaging of the Mark–Houwink coefficients for the copolymers and then appropriate correction against the PMMA standards for the S/AN copolymers and against the PS standards for the *t*BMA/AN copolymers. FTIR spectroscopy (Spectrum BX, Perkin-Elmer, Woodbridge, ON, Canada) was used to determine the molar compositions of the copolymers and the terpolymer. The peak absorbances at 1460, 2200, and 1200 cm^{-1} were used as markers for S, AN, and *t*BMA, respectively. To precisely identify the copolymer compositions, six-point calibration curves were constructed with mixtures of the PS, PAN, and P*t*BMA standards. All of the reactivity ratio determinations were done with samples that were polymerized to low X (<10%) to avoid compositional drift.

RESULTS AND DISCUSSION

Kinetics of poly(S/AN) with a BB initiator

The unimolecular initiator BB (structure shown in Scheme 1) had inherent COOH group functionality, and thus, it could impart a single COOH group at the chain end to be used in reactions with epoxy groups. The first challenge was to understand how AN polymerizations could be controlled via BB. It is important to note that in contrast to TEMPO-mediated systems, unimolecular initiators such as BB can easily control styrenic polymerizations without any additional free-radical initiator. The amount of AN that could be incorporated into the S/AN resins was studied to establish whether the resin would be useful for barrier applications because higher F_{AN}'s (>0.40–0.66) in the copolymer provided better barrier properties.[12] Various S/AN mixtures were synthesized via NMP with BB, with our previous experience with S polymerizations by NMP used as a guide.[44,45] At 90°C in a 50 wt % 1,4-dioxane solution, S/AN mixtures up to an $f_{AN,0}$ of 0.70 were polymerized with BB without any additional SG1 as a mediator. The polymerization rates did not vary significantly as the AN feed content increased, as shown in Figure 1, which represents the semilogarithmic plot of scaled X [$\ln(1 - X)^{-1}$ versus time. Note that the apparent rate constant ($\langle k_p \rangle$[P·], where $\langle k_p \rangle$ is the average propagation rate constant for the copolymerization and [P·] is the concentration of propagating radicals), obtained from the slope in the linear range of Figure 1, decreased slightly from $(5.2 \pm 0.8) \times 10^{-5}$ to $(3.0 \pm 0.2) \times 10^{-5}$ s^{-1} with increasing feed composition ($f_{AN,0} = 0.10$–0.70). This was reasonable because recently published data for the homopropagation rate constant of AN ($k_{p,AN} = 1.1 \times 10^4$ L mol^{-1} s^{-1})[46] suggested that it was nearly an order of magnitude higher compared to the homopropagation rate constant for styrene ($k_{p,S} = 1.8 \times 10^3$ L mol^{-1} s^{-1}) at 90°C.[47] However, the K (the equilbrium constant between dormant and active chains) values between the dormant and active SG1-capped chains were not dissimilar, as determined on the basis of literature estimates. For the S homopolymerizations, $K_S = 4 \times 10^{-10}$ mol/L at 90°C,[48] whereas Nicolas et al.[34] used the K for *n*-butyl acrylate[48] to estimate K for acrylonitrile as $K_{AN} = 1 \times 10^{-11}$ mol/L.

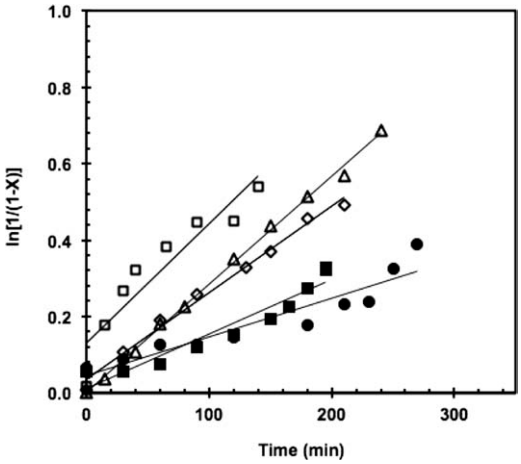

Figure 1 Kinetic plots of the S/AN copolymerization reactions with BB at 90°C in 50 wt % 1,4-dioxane as a function of $f_{AN,0}$: $f_{AN,0}$ = (□) 0.10, (△) 0.30, (◇) 0.40, (■) 0.50, and (●) 0.70. The slopes from the linear regions provided the $\langle k_p \rangle$[P·] values.

The combination of $\langle k_p \rangle$, and the average K, $\langle K \rangle$, for the S/AN copolymerizations suggested that they offset each other, and this combined effect can be neatly summarized by the following equations to

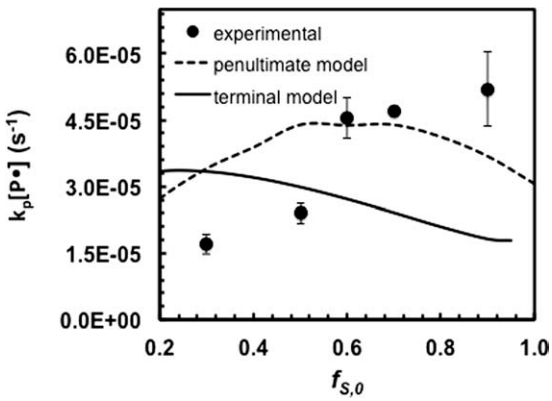

Figure 2 $\langle k_p \rangle$[P·] values for the S/AN copolymerization versus the initial styrene molar feed composition ($f_{S,0}$) with BB at 90°C in 50% 1,4-dioxane solution. The dashed lines indicate the penultimate model prediction for $\langle k_p \rangle$[P·].

predict $\langle k_p \rangle$[P·] from the literature data. The kinetics of free-radical polymerizations are often best described by penultimate kinetic models, and sufficient data was available for S/AN conventional radical copolymerizations to make reasonable predictions. The $\langle k_p \rangle$ based on the implicit penultimate model is given by[49]

$$\langle k_p \rangle = \frac{r_{AN} f_{AN}^2 + 2 f_{AN} f_S + r_S f_S^2}{r_{AN} \frac{f_{AN}}{\overline{k_{p,AN}}} + r_S \frac{f_S}{\overline{k_{p,S}}}} \quad (1)$$

where

$$\overline{k_{p,AN}} = k_{p,AN} \frac{r_{AN} f_{AN} + f_S}{r_{AN} f_{AN} + \frac{f_S}{s_{AN}}}; \quad \overline{k_{p,S}} = k_{p,S} \frac{r_S f_S + f_{AN}}{r_S f_S + \frac{f_{AN}}{s_S}} \quad (2)$$

where r_{AN} and r_S are the monomer reactivity ratios for AN and S, respectively, and s_{AN} and s_S are the radical reactivity ratios for AN and S, respectively. The molar feed fractions for AN and S are given by the acrylonitrile molar feed composition (f_{AN}) and styrene molar feed composition (f_S) = 1 − f_{AN}, respectively. The concentration of propagating macroradicals for a system controlled by persistent free radicals such as SG1 is given by Fischer's expression:[50]

$$[P\cdot] = \left(\frac{\langle K \rangle [I]_0}{3 \langle k_t \rangle} \right)^{1/3} t^{-1/3} \quad (3)$$

where $[I]_0$ is the initial concentration of the BB nitroxide initiator, $\langle k_t \rangle$ is the average termination rate constant, and $\langle K \rangle$ is the average equilibrium constant for the implicit penultimate model derived by Charleux et al:[51]

$$\langle K \rangle = \frac{\frac{r_{AN} f_{AN}}{\overline{k_{p,AN}}} + \frac{r_S f_S}{\overline{k_{p,S}}}}{\frac{r_{AN} f_{AN}}{\overline{k_{p,AN}} K_{AN}} + \frac{r_S f_S}{\overline{k_{p,S}} K_S}} \quad (4)$$

$\langle k_t \rangle$ for the penultimate copolymerization model is given by[52]

$$\langle k_t \rangle = \left(p_S k_{t,S}^{1/2} + p_{AN} k_{t,AN}^{1/2} \right)^2 \quad (5)$$

where $k_{t,S}$ and $k_{t,AN}$ are the homotermination rate constants for S and AN, respectively, and p_S and p_{AN} are given by

$$p_S = \frac{\frac{r_S f_S}{\overline{k_{p,S}}}}{\frac{r_S f_S}{\overline{k_{p,S}}} + \frac{r_{AN} f_{AN}}{\overline{k_{p,AN}}}} \quad \text{and} \quad p_{AN} = 1 - p_S \quad (6)$$

The $k_{t,S}$ at 90°C was taken from Beuermann and Buback[53] to be 1.3 × 10^8 L mol^{-1} s^{-1} whereas $k_{t,AN}$ was taken from the expression provided by Keramopoulos and Kiparissides[54] with $k_{t,AN} = 1.98 \times 10^{14} \times e^{-5400/RT}$ [where R is the gas constant and T is the temperature (K)] to give $k_{t,AN}$ (90°C) = 9.2 × 10^9 L mol^{-1} s^{-1}. The only other parameters required were the monomer and radical reactivity ratios for the penultimate model, which were taken from Hill et al.[55] from data at 60°C (because data at 90°C was not available): $r_S = 0.22$, $r_{AN} = 0.039$, $s_S = 0.634$, and $s_{AN} = 0.229$. Given this literature data and the previous expressions, a predicted $\langle k_p \rangle$[P·] for the S/AN nitroxide-mediated copolymerization could be compared to the experimental data. Note that [P·] was estimated as the steady state was approached, typically after a polymerization time of about 5 × 10^2 s^{-1}, where the change in [P·] was negligible. The experimental results and the predicted $\langle k_p \rangle$[P·] values are plotted as a function of f_S in Figure 2. Note that the predicted data did not match the experimental data very closely, but in either case, the variation of $\langle k_p \rangle$[P·] with composition was not wide.

The molecular weights obtained via GPC were used in conjunction with the kinetic data to obtain plots of M_n versus monomer conversion (X). Such plots were used to evaluate the control of the polymerization for the CRP processes, particularly to see if the polymerization approached the linear behavior indicative of truly living polymerizations. The copolymers exhibited narrow MWDs and appeared monomodal in nature (Fig. 3) with low polydispersities (M_w/M_n = 1.17–1.26), suggestive of controlled polymerizations. Figure 4 shows the plot of M_n versus X for the BB-controlled S/AN copolymerizations at various $f_{AN,0}$ values. Note that the straight, solid line is the theoretically expected M_n versus X behavior. Note that there was some uncertainty in the estimation of M_n because the corrections may not have been available at the temperature used for the GPC. Still, the plots were relatively linear up to about X = 0.4 ($M_n \approx$ 16.0 kg/mol); this suggested that pseudo-living behavior was approached up to that point.

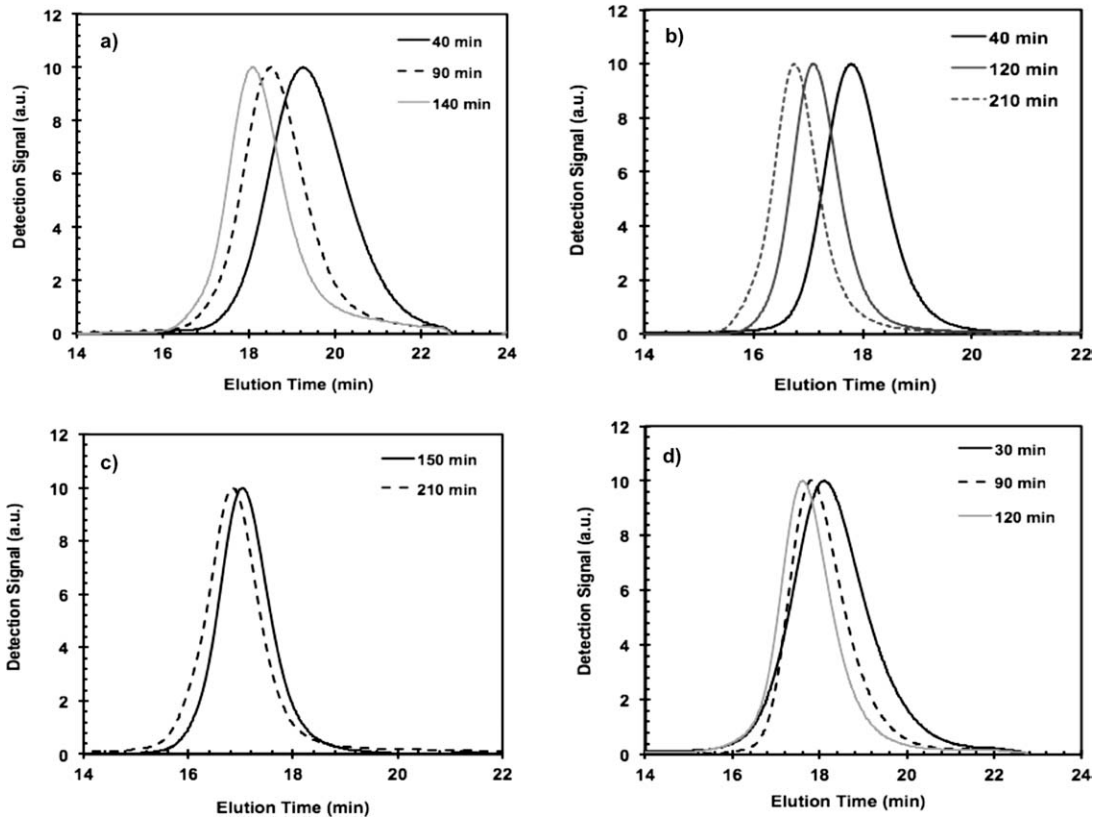

Figure 3 Gel permeation chromatograms of samples taken at various times for the S/AN copolymerizations performed in a 50 wt % 1,4-dioxane solution at 90°C with an $M_{n,\text{target}}$ value of 25 kg/mol and with different monomer feed concentrations with the BB initiator: (a) S/AN–BB-10 ($f_{\text{AN},0} = 0.10$), (b) S/AN–BB-30 ($f_{\text{AN},0} = 0.30$), (C) S/AN–BB-50 ($f_{\text{AN},0} = 0.50$), and (d) S/AN–BB-70 ($f_{\text{AN},0} = 0.70$).

The characteristics of the final S/AN copolymers controlled with BB are displayed in Table III.

Kinetics of poly(tBMA-*ran*-AN) with a BB initiator

Before the synthesis of S/AN copolymers with COOH functionality at random locations along the chain length were done, it was necessary to understand how the copolymer feed composition controlled the reactivity and kinetics in each of the following binary systems: S/AN, *t*BMA/S, and *t*BMA/AN copolymers. *t*BMA/S copolymers synthesized with BB were reported by our research group[45] under the same conditions used in this

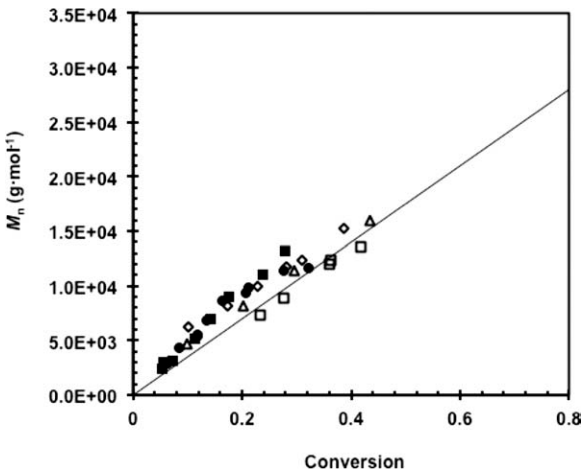

Figure 4 M_n versus X for the S/AN copolymerizations performed in a 50 wt % 1,4-dioxane solution at 90°C with an $M_{n,\text{target}}$ of 25 kg/mol with BB with various $f_{\text{AN},0}$'s: (□) 0.10, (△) 0.30, (◇) 0.40, (■) 0.50, and (●) 0.70.

TABLE III
Summary of the Compositions and Molecular Weight Characteristics of Poly(S/AN)s Initiated from BB in Dioxane at 90°C

Experiment ID[a]	$f_{\text{AN},0}$	F_{AN}[b]	X	M_n (kg/mol)[c]	M_w/M_n[c]
S/AN–BB-10	0.10	0.22	0.42	13.6	1.23
S/AN–BB-30	0.30	0.38	0.43	16.0	1.17
S/AN–BB-40	0.40	0.44	0.40	15.3	1.18
S/AN–BB-50	0.50	0.46	0.28	13.2	1.18
S/AN–BB-70	0.70	0.52	0.32	10.7	1.26

[a] All of the S/AN copolymerizations were done in 50 wt % 1,4-dioxane at 90°C.
[b] The copolymer composition was determined with FTIR spectroscopy.
[c] M_w, M_n, and M_w/M_n were determined with GPC relative to linear PMMA standards in DMF at 50°C after correction with composition-averaged Mark–Houwink parameters of poly(S/AN) in DMF.

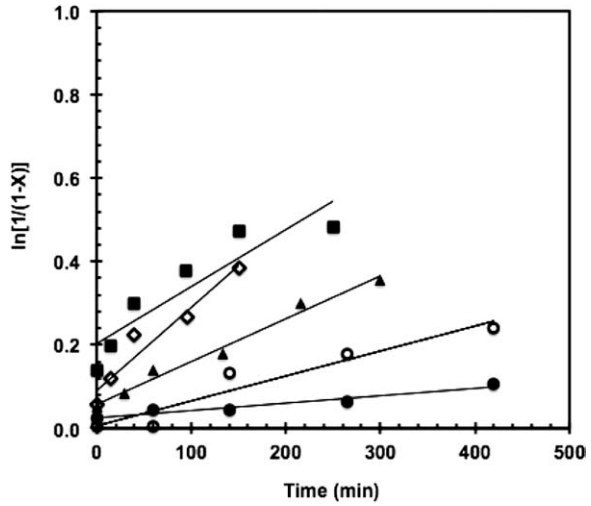

Figure 5 Kinetic plots of the *t*BMA/AN copolymerizations with BB/SG1 (r = 8.1–8.5 mol %) at 90°C in 50 wt % 1,4-dioxane as a function of $f_{AN,0}$: $f_{AN,0}$ = (◇) 0.11, (■) 0.30, (▲) 0.51, (○) 0.70, and (●) 0.80. The slopes from the linear regions provided the $\langle k_p \rangle$[P·] values.

study. In the previous section, we explored S/AN copolymerization using the carboxylic acid terminated BB initiator. The results with *t*BMA/AN would complete the examination of the three binary NMP systems, which would be relevant for the subsequent tailoring of terpolymers for functional S/AN-based barrier materials with random methacrylic acid groups.

*t*BMA/AN copolymers were synthesized with BB initiator with an excess of SG1 (8.1–8.5 mol % SG1 relative to BB) for $f_{AN,0}$ values from 0.11–0.80 in 50 wt % dioxane solutions at 90°C. The excess SG1 was used to provide a sufficient concentration of the persistent radical to control the methacrylate-rich polymerization.[34,44,45,51,56] Figure 5 shows the first-order kinetic plots of $\ln(1 - X)^{-1}$ versus time for the *t*BMA/AN copolymerizations with BB/SG1. For all plots, X increased with a relatively linear trend up to about a 50% scaled X (depending on the AN feed composition); this implied a constant radical concentration and suggested a controlled polymerization. Extraction of the $\langle k_p \rangle$[P·] values from the slopes indicated that increasing AN feed concentration tended to decrease the polymerization rate from $(3.3 \pm 0.5) \times 10^{-5}$ to $(5.1 \pm 0.3) \times 10^{-6}$ s^{-1}. When excess SG1 was used, the $\langle k_p \rangle$[P·] values could be converted into the product of $\langle k_p \rangle \langle K \rangle$, which combined the two key features controlling the NMP process. Given the definition of $\langle K \rangle$ as the ratio of the concentration of active species ([P·] and concentration of free nitroxide [SG1]) to that of the dormant species (concentration of SG1-capped macroradicals [P-SG1]), $\langle k_p \rangle \langle K \rangle$ could be written as eq. (7), provided some assumptions are applied:

$$\langle k_p \rangle \langle K \rangle = \langle k_p \rangle \frac{[\mathrm{SG1}][\mathrm{P}\cdot]}{[\mathrm{P} - \mathrm{SG1}]} \approx \langle k_p \rangle \frac{[\mathrm{SG1}]_0[\mathrm{P}\cdot]}{[\mathrm{BB}]_0} = \langle k_p \rangle [\mathrm{P}\cdot] r \tag{7}$$

First, it was assumed that SG1 was added at a sufficiently high concentration so that it did not vary much during the course of polymerization so that [SG1] ≈ initial SG1 concentration $[SG1]_0$. Also, [P-SG1] ≈ $[BB]_0$ when the chains remained relatively pseudo-living; this held approximately true during the early stages of the polymerization, where the $\ln[(1 - X)^{-1}]$ versus time plots were linear. This was later further verified by the linear M_n versus X plots for the copolymerization in the X ranges studied. Given these assumptions, eq. (7) could be written with $\langle k_p \rangle \langle K \rangle$, as a function of the $\langle k_p \rangle$[P·] values from the slopes of the kinetic plots in Figure 5 and the molar concentration ratio of the initial free nitroxide to BB, given as $r = [SG1]_0/[BB]_0$.

The experimental estimates of $\langle k_p \rangle \langle K \rangle$ for the *t*BMA/AN copolymerizations are plotted as a function of $f_{AN,0}$ in Figure 6. Unlike the S/AN copolymerization described in the previous section, $\langle k_p \rangle \langle K \rangle$ dropped much more steeply with increasing AN content in the feed. As noted previously, Junkers et al.[46] recently reported data for $k_{p,AN} = 1.1 \times 10^4$ L mol^{-1} s^{-1}; this implies that it was between 0.5 to 1 order of magnitude higher compared to the homopropagation rate constant of *t*BMA ($k_{p,tBMA} = 1.6 \times 10^3$ L mol^{-1} s^{-1}) at 90°C.[57] However, there was a larger discrepancy between the K values of the two species. Nicolas et al.[34] took $K_{AN} \approx$ the equibrium constant for butyl acrylate = $K_{BA} = 1 \times 10^{-11}$ mol/L. K_{tBMA} was not measured, but it was estimated to be similar to that of the structurally related MMA ($K_{tBMA} \approx 2.6 \times 10^{-7}$ mol/L).[45]

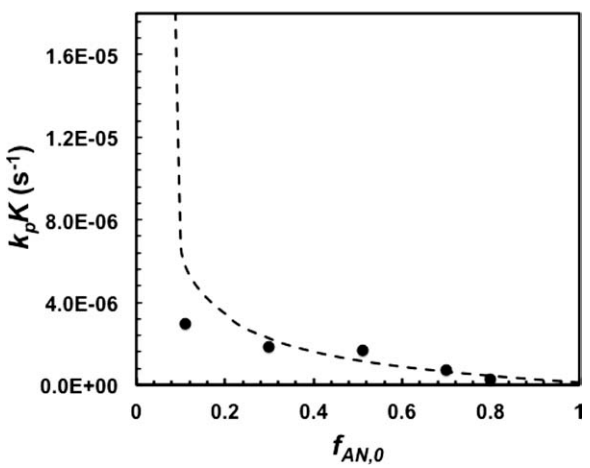

Figure 6 Product of $\langle k_p \rangle \langle K \rangle$ for the *t*BMA/AN copolymerizations versus $f_{AN,0}$ with BB/SG1 at 90°C in a 50% 1,4-dioxane solution. The dashed line indicates the prediction based on the terminal model for $\langle k_p \rangle \langle K \rangle$.[51]

TABLE IV
Summary of the Compositions and Molecular Weight Characteristics of Poly(*t*BMA-*ran*-AN) Copolymers Initiated from BB/SG1 in Dioxane at 90°C

Experiment ID[a]	$f_{AN,0}$	F_{AN}[b]	X	M_n (kg/mol)[c]	M_w/M_n[c]
*t*BMA/AN–BB/SG1-11	0.11	0.12	0.66	14.8	1.40
*t*BMA/AN–BB/SG1-30	0.30	0.22	0.57	11.9	1.35
tBMA/AN–BB/SG1-51	0.51	0.27	0.51	11.4	1.33
*t*BMA/AN–BB/SG1-70	0.70	0.34	0.32	5.0	1.24
*t*BMA/AN–BB/SG1-80	0.80	0.37	0.20	4.7	1.17

[a] All of the *t*BMA/AN copolymerizations were done in 50 wt % 1,4-dioxane at 90°C. *t*BMA/AN–BB-*xx* refers to *t*BMA/AN copolymerizations done with BB/SG1 and *xx* refers to the molar feed composition with respect to AN.
[b] The copolymer composition was determined with FTIR spectroscopy.
[c] M_w, M_n, and M_w/M_n determined with GPC relative to linear PS standards in THF at 40°C.

Because data required for the *t*BMA/AN copolymerization was scarce and the only reactivity ratios known for this particular pair were those derived from our study ($r_{AN} = 0.14 \pm 0.03$ and $r_{tBMA} = 0.89 \pm 0.19$), the predicted $\langle k_p \rangle \langle K \rangle$ for the *t*BMA/AN assumed a terminal model for the kinetics, and the expression derived by Charleux et al.[51] for such a model was subsequently used to compare against our experimental data:

$$\langle k_p \rangle \langle K \rangle = \frac{r_{AN} f_{AN}^2 + 2 f_{AN} f_{tBMA} + r_{tBMA} f_{tBMA}^2}{r_{AN} \frac{f_{AN}}{k_{p,AN} K_{AN}} + r_{tBMA} \frac{f_{tBMA}}{k_{p,tBMA} K_{tBMA}}} \quad (8)$$

where f_{AN} and f_{tBMA} are the feed fractions for AN and *t*BMA, respectively. In Figure 6, there was reasonable agreement between the experimental data and the predicted $\langle k_p \rangle \langle K \rangle$ in the feed composition range studied. More rigorous testing of the model would require examination of much lower AN feed compositions, where there was a dramatic increase in $\langle k_p \rangle \langle K \rangle$ expected. However, our motivation was focused toward the use of higher AN feed compositions because we ultimately desire to use AN to impart more favorable barrier properties.

The molecular weight characteristics were determined by GPC relative to linear PS standards in THF solvent at 40°C. It should be noted that because the highest AN incorporation was 37 mol % in the final copolymer (experiment ID *t*BMA/AN–BB/SG1–80 in Tables II and IV), the samples were easily soluble in THF. Note that Mark–Houwink parameters were not available for poly(AN) in THF, so the corrections were not ideal. However, GPC analysis for the *t*BMA/AN experiments revealed monomodal MWDs with relatively low M_w/M_n values (1.17–1.40) that were suggestive of a controlled polymerization. The GPC traces shown in Figure 7 displayed a leftward shift in the MWD; this indicated a steady, monomodal growth in the copolymer chains over time. M_n versus X plots (Fig. 8) were linear up to about 55% X ($M_n = 14.8$ kg/mol) for the different AN feed compositions; this indicated that pseudoliving behavior was approached up to that point. In some cases, the M_n values began to slightly plateau at high Xs; this indicated that some irreversible termination reactions have occurred. The molecular weight characteristics and final copolymer compositions are summarized in Table IV.

Chain extensions were also done in the case of the two macroinitiators with AN concentrations of about 50 mol % to see whether block copolymers could be formed. The molecular weights of the macroinitiators were relatively high, and thus, it was difficult

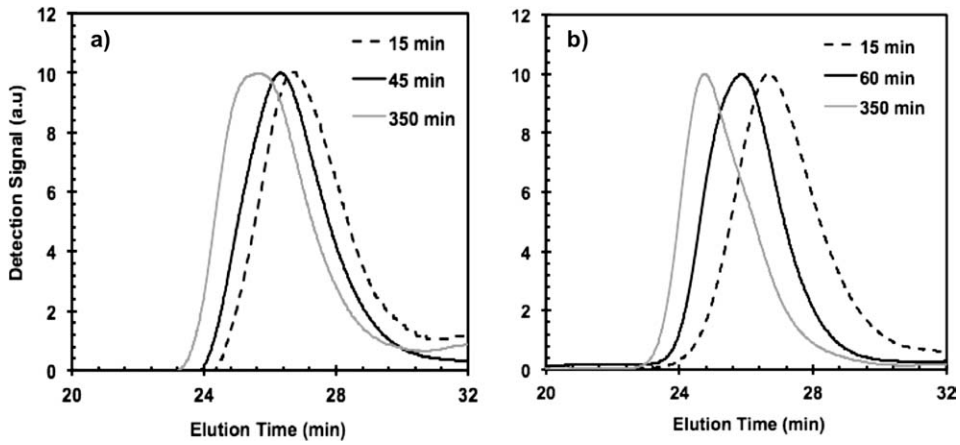

Figure 7 Gel permeation chromatograms of samples taken at various times for the *t*BMA/AN copolymerizations performed in 50 wt % 1,4-dioxane at 90°C with an $M_{n,target}$ value of 25 kg/mol and with different monomer feed concentrations with the BB/SG1 initiator. The experiments are denoted as *t*BMA/AN–BB/SG1-*xx*, where *xx* represents the initial molar feed concentration of AN given by $f_{AN,0}$: (a) *t*BMA/AN–BB/SG1-11 ($f_{AN,0} = 0.11$) and (b) *t*BMA/AN–BB/SG1-30 ($f_{AN,0} = 0.30$). The GPC was performed in THF at 40°C with PS standards.

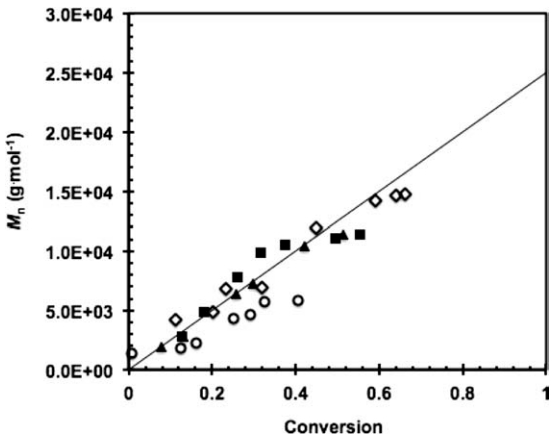

Figure 8 M_n versus X for the *t*BMA/AN copolymerizations performed in a 50 wt % 1,4-dioxane solution at 90°C with an $M_{n,\text{target}}$ value of 25 kg/mol with BB/SG1 at various AN feed compositions.

for us to apply NMR for chain-end fidelity with a high degree of certainty. The simplest method to apply for observing whether there was sufficient SG1 at the chain end was the addition of a second batch of monomer and observation of the GPC traces of the product after addition. Figure 9 shows the GPC traces for the S/AN macroinitiator and the product after addition of a second S/AN batch after 270 min at 115°C [Fig. 9(a)] and the *t*BMA/AN macroinitiator and the product after the addition of a second *t*BMA/AN batch after 225 min of polymerization at 90°C [Fig. 9(b)]. In both cases, a clear shift in the MWD was observed; this indicated that a sufficiently high concentration of SG1 groups was available on the chain terminus to produce block copolymers. In the case of the S/AN copolymers, shown in Figure 9(a), some dead macroinitiator ($\sim$ 20%) was clearly observed in the macroinitiator trace; this was not surprising because the initial polymerization was done to quite a high X. Consequently, the dead macroinitiator remained, and M_w/M_n was quite high for the chain-extended species ($M_w/M_n = 1.68$). In the case of the *t*BMA/AN chain extensions from the tBMA/AN macroinitiator, shown in Figure 9(b), the GPC traces clearly showed steady monomodal shifts to higher molecular weights and a final M_w/M_n of 1.37. Thus, the AN-containing copolymers served as relatively effective macroinitiators for the addition of a second batch of monomer.

Copolymer composition

The copolymer composition with respect to monomer 1 (F_1) may have been quite different from that of the feed composition of monomer 1 (f_1). The copolymer composition could be obtained from well-known relationships, such as the Mayo–Lewis equation,[58] shown in eq. (9), which requires the knowledge of the monomer reactivity ratios,[59–61] r_1 and r_2, that describe the preference of monomer 1 for attaching to a chain with a terminal unit of 1 relative to a terminal unit of 2 (r_1) and the preference of monomer 2 for attaching to a chain with a terminal unit of 2 relative to a terminal unit of 1 (r_2):

$$F_1 = \frac{r_1 f_1^2 + f_1(1-f_1)}{r_2(1-f_1)^2 + 2f_1(1-f_1) + r_1 f_1^2} \tag{9}$$

The copolymer compositions were initially predicted in terms of the initial monomer concentrations with Mayo's terminal copolymerization model[58] and the assumption that the active site reactivity depended on the nature of the reactive terminus. The monomer reactivity ratios for S/AN and

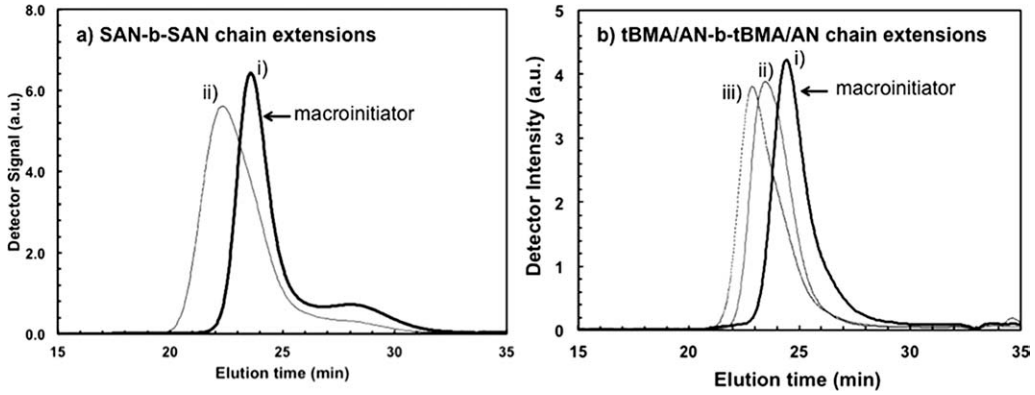

Figure 9 GPC of the (a) poly(S/AN) macroinitiator [(i) ID = S/AN–BB-50, $M_n = 13.2$ kg/mol, and $M_w/M_n = 1.18$ (see Table III for a full characterization of the macroinitiator) with an equimolar batch of S/AN to form the chain-extended product after 270 min at 90°C in 50 wt % dioxane solution and (ii) $M_n = 23.4$ kg/mol and $M_w/M_n = 1.68$] and (b) poly (*t*BMA-*ran*-AN) macroinitiator [(i) (ID = *t*BMA/AN–BB/SG1-50, $M_n = 11.4$ kg/mol, and $M_w/M_n = 1.33$ (see Table IV for a full characterization of the macroinitiator) chain-extended with an equimolar batch of *t*BMA/AN after 95 min, (ii) $M_n = 19.1$ kg/mol and $M_w/M_n = 1.32$, and (iii) after 225 min ($M_n = 24.4$ kg/mol and $M_w/M_n = 1.37$) polymerization at 90°C in a 50 wt % dioxane solution].

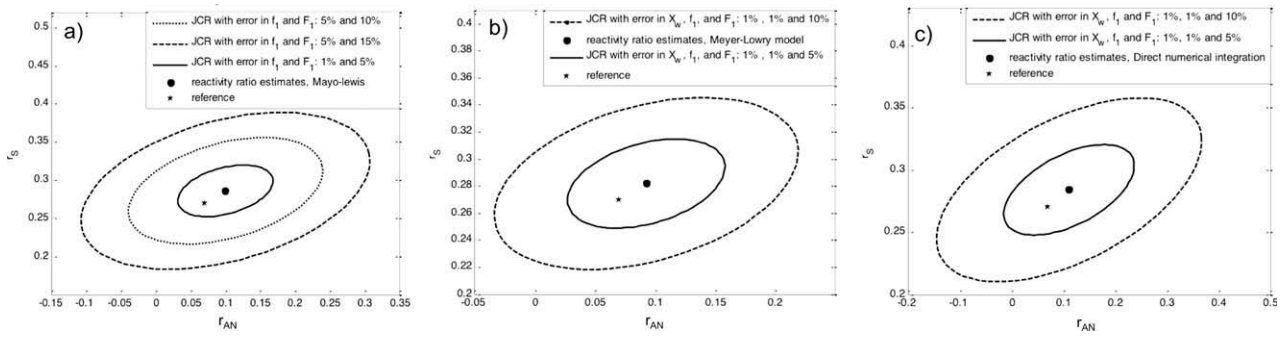

Figure 10 Reactivity ratio estimates for the S/AN copolymerizations (r_S = reactivity ratio of styrene and r_{AN} = reactivity ratio of acrylonitrile) with the BB initiator at 90°C in a 50 wt % dioxane solution with various models. (a) The reactivity ratio plot with three different JCRs for different errors in f_1 and F_1 (1 = AN). The reactivity ratios determined by the Fineman–Ross method were used as a reference. The reactivity ratios estimated with the EVM are indicated by the black circles. (b) The reactivity ratios were determined on the basis of the Meyer–Lowry model with the Fineman–Ross estimates as initial guesses for the reactivity ratios. Two JCRs were indicated in the plot for errors in f_1 and F_1. (c) The reactivity ratios determined by a direct numerical integration of the Mayo–Lewis equation with the Fineman–Ross estimates as initial guesses. Two JCRs were indicated in the plot for errors in f_1 and F_1. X_w denotes X.

*t*BMA/AN were also fit with the Kelen–Tüdos method[60,61] and were then also revisited by improved estimation techniques, such as the error-in-variables model (EVM), with instantaneous composition[62] or via a direct numerical integration of the cumulative composition,[63] or with the Meyer–Lowry model,[64] which provided more reliable estimates of the reactivity ratios.

For conventional radical polymerization, the reactivity ratios for S/AN copolymerizations are well known. The reactivity ratios may be slightly different for CRPs because the retardation of the termination processes results in chains with much higher chain-to-chain compositional homogeneity compared to conventional radical polymerizations. For example, Fan et al.[16] reported an r_{AN} of 0.19 and an r_S of 0.46 for S/AN copolymerization by reversible addition–fragmentation chain-transfer polymerization; these values were slightly higher than those reported by conventional radical polymerization. They attributed the difference to the different affinity of the propagating chain end with the dithioester chain-transfer agent used. The reactivity ratios for the S/AN copolymerizations with BB were $r_{AN} = 0.07 \pm 0.01$ and $r_S = 0.27 \pm 0.02$ (Fineman–Ross method) and $r_{AN} = 0.10 \pm 0.01$ and $r_S = 0.28 \pm 0.02$ (Kelen–Tüdos method). Conventional radical copolymerization of S/AN provided reactivity ratios of r_{AN} = 0.04–0.06 and r_S = 0.47–0.54[65] and $r_{AN} = 0.053$ and $r_S = 0.331$.[55] Thus, the reactivity ratios that we determined were closer to those reported by conventional radical polymerization than to those reported by Fan et al.;[19] this suggested that the activity of the chain end was not as strongly altered by the nitroxide as it was by the dithioester.

We also employed the EVM method to estimate the reactivity ratios for S/AN because such a method can take into account the effect of the error in all variables (both dependent and independent), including the effect of X. As shown in Figure 10(a), when the Mayo–Lewis model was applied for the two larger error levels, r_{AN} crossed the $r_{AN} = 0$ line, and the joint confidence regions (JCRs) went to the negative region; this reflected a high degree of uncertainty in the estimation results for r_{AN}. This could have been partly related to the fact that in the data set used, the X values were as high as 23%; this was not appropriate for the Mayo–Lewis model.

Moreover, the $f_{AN,0}$ values of the data set were over the range 0.1–0.7 for AN. According to the Tidwell–Mortimer D-optimal design criterion for reactivity ratio estimation,[66,67] the experiments should have been run at the two optimal feed compositions of 0.119 and 0.966 for AN, on the basis of starting guesses of $r_{AN} = 0.07$ and $r_S = 0.27$. The first optimal point was very close to the first data point, which was very rich in S. However, the second optimal point was not included in the data set, and this could have been another reason that we obtained more reliable results for r_S compared to r_{AN}.

One can also see in Figure 10(b) for the Meyer–Lowry model and in Figure 10(c) for the direct numerical integration approach that r_{AN} crossed the zero line, and therefore, the JCRs when through the negative region, with the exception of only the lowest error level and only for the Meyer–Lowry model analysis. Compared to those in Figure 10(a), the results in Figure 10(b,c) were more reliable, as they were based on cumulative composition models and, thus, took into account the effect of the X level as well.

We also conducted the following exercise to check the trend in obtaining point estimates. We used the three low X points (X = 0.073, 0.084, and 0.10), obtained estimates from low-X data (Mayo–Lewis),

TABLE V
Summary of the Reactivity Ratio Estimates for the S/AN Copolymerizations Initiated with BB at 90°C in Dioxane

Model	Comment	r_{AN}	r_S	Description
Reference (Fineman–Ross)	Instantaneous model, X values are not included	0.07 ± 0.01	0.27 ± 0.02	Error bars estimated from the slope and intercept of the plot
Mayo–Lewis (EVM)	Instantaneous model, X values are not included	0.099	0.286	JCR for three different error levels are shown in Figure 10(a)
Meyer–Lowry (EVM)	Cumulative model, X values are included	0.093	0.282	JCR for two different error levels are shown in Figure 10(b)
Direct numerical integration (EVM)	Cumulative model, X values are included	**0.111**	**0.284**	JCR for two different error levels are shown in Figure 10(c)

and then used the higher X data ($X = 0.10$, 0.17, and 0.23) to obtain estimates but with cumulative composition data. The obtained estimates were very close (if not identical) to the estimates highlighted in bold in Table V (i.e., the ones with the direct numerical integration, which we believe is a more reliable approach because it considers information from composition data at both low- and high-X regimes[63]). The reactivity ratios are summarized in the Mayo plots shown in Figure 11, which indicate the copolymer composition expected for a given feed. Note that the azeotropic composition at about 40 mol % AN was still attained; this was in agreement with previous studies.

The *t*BMA/AN reactivity ratios for BB/SG1 controlled polymerizations were $r_{AN} = 0.07 \pm 0.01$ and $r_{tBMA} = 1.24 \pm 0.20$ (Fineman–Ross method) and $r_{AN} = 0.14 \pm 0.03$ and $r_{tBMA} = 0.89 \pm 0.19$ (Kelen–Tüdos method). We attempted to use these values as initial guesses to obtain better estimates of the reactivity ratios using EVM. Figure 12 shows the Mayo–Lewis model prediction of F_{AN} versus f_{AN} with the reference reactivity ratios, along with experimental data. The purpose of creating this plot was to check whether the experimental points deviated from the trend shown by the Mayo–Lewis line or not because one of the main reasons for meaningless results (negative reactivity ratio) could be high experimental error. Several scenarios were tried to check whether a positive r_{AN} could be estimated.

First, we assumed that there was no error in the data; the estimation results still yielded a negative r_{AN}. Second, both the nonlinear least-squares and EVM methods were used, and still, the estimation results indicated the possibility of a negative r_{AN}. Finally, a Q–e (Q = reactivity of monomer and e = polarity interaction of radical and molecule) scheme was used to check the region of initial guesses for reactivity ratios with the Q–e data available for AN and butyl methacrylate (BMA; structurally related to *t*BMA; we used this because data for *t*BMA was not available; reactivity of AN monomer = $Q_{AN} = 0.48$, polarity interaction of AN = $e_{AN} = 1.23$, reactivity of BMA monomer = $Q_{BMA} = 0.82$, polarity interaction of BMA = $e_{BMA} = 0.28$); this gave values of $r_{AN} = 0.18$ and $r_{BMA} = 2.23$.[68]

Even with these new initial guesses, we still obtained negative results for r_{AN}. In addition, the new reactivity ratios were used to produce the Mayo–Lewis plot, and like that in Figure 12, the

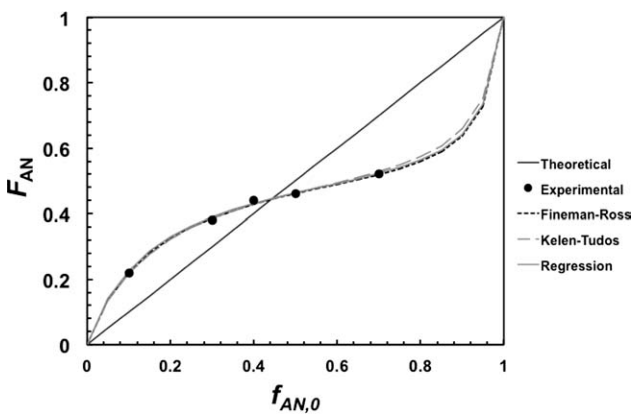

Figure 11 Mayo plot indicating F_{AN} versus $f_{AN,0}$ for the S/AN copolymerizations with BB at 90°C in 1,4-dioxane. The straight line through the origin is the azeotropic composition. A nonlinear regression fit to the Mayo equation was also done and provided similar fits to the data as the Fineman–Ross and Kelen–Tüdos fits.

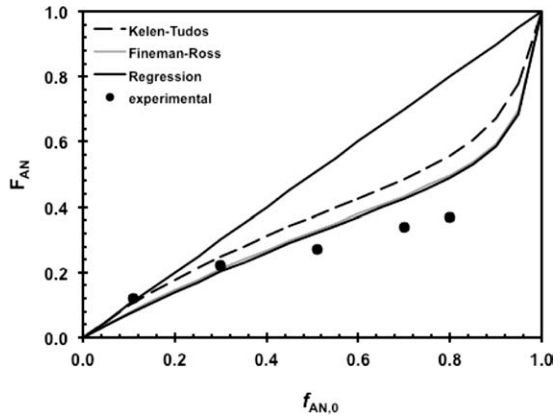

Figure 12 Mayo plot showing F_{AN} versus $f_{AN,0}$ for the *t*BMA/AN copolymers with BB/SG1 at 90°C in 1,4-dioxane. A nonlinear regression fit to the Mayo equation was also performed and provided similar results to the Kelen–Tüdos fit of the data. The reactivity ratio estimates from the EVM suggested that the experimental data possessed considerable uncertainty.

experimental trend and the predicted line did not match well. This, again, could have pointed to experimental data with significant error. Because it is well known that AN can precipitate or phase separate from its polymer during polymerization[69–72] it was possible that the calculated AN composition was higher than it actually was. In summary, the data suggest that the experimental uncertainty was quite high, and future experiments will be done with replicates and design of experiments to obtain more reliable reactivity ratios.

We could, however, compare the *t*BMA/AN reactivity ratios we obtained to similar methacrylate/AN systems that were determined by similar methods. For example, Nair and Muthana[73] reported isobutyl methacrylate (i-BMA)/AN reactivity ratios from conventional radical copolymerization of $r_{AN} = 0.21$ and $r_{i\text{-BMA}} = 1.04$ and BMA/AN reactivity ratios of $r_{AN} = 0.30$ and $r_{BMA} = 1.08$, whereas Kapur and Brar[74] reported values of $r_{AN} = 0.30$ and $r_{BMA} = 1.08$, and Greenley[75] reported values of $r_{AN} = 0.29$ and $r_{BMA} = 0.98$. Khesareh et al.[71] reported MMA/AN reactivity ratios of $r_{AN} = 0.15$ and $r_{MMA} = 1.04$, whereas El-Sabee et al.[76] reported ethyl methacrylate (EMA)/AN reactivity ratios from conventional radical polymerization of $r_{AN} = 0.34 \pm 0.01$ and $r_{EMA} = 0.85 \pm 0.12$. Thus, the *t*BMA/AN reactivity ratios agreed reasonably well with those reported by the conventional radical polymerizations of related alkyl methacrylate/AN copolymerizations. Of course, our own analysis suggested that more data must be obtained to get better estimates of the reactivity ratios, and we are presently designing experiments for the *t*BMA/AN system.

CONCLUSIONS

S/AN resins ($f_{AN,0} = 0.10$–0.86) were synthesized with a BB unimolecular initiator at 90°C in a controlled manner with a narrow MWD ($M_w/M_n = 1.14$–1.26) and relatively linear M_n versus X plots ($M_n = 15.3$–18.1 kg/mol, $X = 40$–70%). The incorporation of AN into styrenic resins was possible at relatively high loadings, in some cases up to about 52 mol %. AN-containing resins with potential random carboxylic acid functionality were derived with the protected form of methacrylic acid, *t*BMA, in a copolymerization with AN with BB/SG1 at 90°C. For $f_{AN,0} = 0.10$–0.80, the *t*BMA/AN copolymers exhibited a relatively narrow MWD ($M_w/M_n = 1.17$–1.40) and linear M_n versus X plots ($M_n = 14.8$ kg/mol, $X = 55\%$). The reactivity ratios were $r_{AN} = 0.07 \pm 0.01$ and $r_S = 0.27 \pm 0.02$ (Fineman–Ross) and $r_{AN} = 0.10 \pm 0.01$ and $r_S = 0.28 \pm 0.02$ (Kelen–Tüdos) for the S/AN copolymerizations; this was in good agreement with conventional radical polymerizations. For the *t*BMA/AN copolymerizations, we obtained values of $r_{AN} = 0.07 \pm 0.01$ and $r_{tBMA} = 1.24 \pm 0.20$ (Fineman–Ross) and $r_{AN} = 0.14 \pm 0.03$ and $r_{tBMA} = 0.89 \pm 0.19$ (Kelen–Tüdos); these were similar to data from related alkyl methacrylate/AN conventional radical copolymerizations. These results suggest that terminal and pendant carboxylic acid functional AN copolymers can be synthesized in a controlled manner with BB-type unimolecular initiators.

The authors thank Scott Schmidt and Noah Macy of Arkema, Inc., for their aid in obtaining the BB and SG1 used in this work.

References

1. Yeh, J.-T.; Yao, W.-H.; Chen, C.-C. J Polym Res 2005, 12, 279.
2. Yeh, J.-T.; Huang, S.-S.; Yao, W.-H. Macromol Mater Eng 2002, 287, 532.
3. Yeh, J.-T.; Fan-Chiang, C.-C. J Polym Res 1996, 3, 211.
4. Harrats, C.; Dedecker, K.; Groeninckx, G.; Jérôme, R. Macromol Symp 2003, 198, 183.
5. Halldén, A.; Ohlsson, B.; Wesslén, B. J Appl Polym Sci 2000, 78, 2416.
6. Ashcraft, E.; Ji, H.; Mays, J.; Dadmun, M. Am Chem Soc Appl Mater Interfaces 2009, 1, 2163.
7. Yin, Z.; Koulic, C.; Pagnoulle, C.; Jérôme, R. Macromolecules 2001, 34, 5132.
8. Sailer, C.; Handge, U. A. Macromolecules 2008, 41, 4258.
9. Orr, C. A.; Cernohous, J. J.; Guegan, P.; Hirao, A.; Jeon, H. K.; Macosko, C. W. Polymer 2001, 42, 8171.
10. Jarus, D.; Hiltner, A.; Baer, E. Polymer 2002, 43, 2401.
11. Jeon, H. K.; Macosko, C. W.; Moon, B.; Hoye, T. R.; Yin, Z. Macromolecules 2004, 37, 2563.
12. Rodriguez, F.; Cohen, C.; Ober, C. K.; Archer, L. A. Principles of Polymer Systems, 5th ed.; Taylor & Francis: New York, 2003.
13. Braunecker, W. A.; Matyjaszewski, K. Prog Polym Sci 2007, 32, 93.
14. Couturier, J.-L.; Guerret, O.; Bertin, D.; Gigmes, D.; Marque, S.; Tordo, P.; Dufils, P.-E. U.S. Pat. 2005/0065119 A1 (2005).
15. Božović-Vukić, J.; Manon, H. T.; Meuldijk, J.; Koning, C.; Klumperman, B. Macromolecules 2007, 40, 7132.
16. Fan, D.; He, J.; Xu, J.; Tang, W.; Liu, Y.; Yang, Y. J Polym Sci Part A: Polym Chem 2006, 44, 2260.
17. Tsarevsky, N. V.; Sarbu, T.; Gobelt, B.; Matyjaszewski, K. Macromolecules 2002, 35, 6142.
18. Pietrasik, J.; Dong, H.; Matyjaszewski, K. Macromolecules 2006, 39, 6384.
19. Shanmuragharaj, A. M.; Bae, J. H.; Nayak, R. R.; Ryu, S. H. J Polym Sci Part A: Polym Chem 2007, 45, 460.
20. Fukuda, T.; Terauchi, T.; Goto, A.; Tsujii, Y.; Miyamoto, T.; Shimizu, Y. Macromolecules 1996, 29, 3050.
21. Baumert, M.; Mulhaupt, R. Macromol Rapid Commun 1997, 18, 787.
22. Hua, F. J.; Chen, S. M.; Lee, D. S.; Yang, Y. L. Appl Magn Reson 2001, 21, 49.
23. Baumann, M.; Roland, A. I.; Schmidt-Naake, G.; Fischer, H. Macromol Mater Eng 2000, 280–281, 1.
24. Baumann, M.; Schmidt-Naake, G. Macromol Chem Phys 2001, 202, 2727.
25. Detrembleur, C.; Sciannamea, V.; Koulic, C.; Claes, M.; Hoebeke, M.; Jerome, R. Macromolecules 2002, 35, 7214.
26. Lokaj, J.; Brozova, L.; Holler, P.; Pientka, Z. Collect Czech Chem Commun 2002, 67, 267.

27. Benoit, D.; Chaplinski, V.; Braslau, R.; Hawker, C. J. J Am Chem Soc 1999, 121, 3904.
28. Chen, Q.; Zhang, Z.; Zhou, N.; Cheng, Z.; Tu, Y.; Zhu, X. J Polym Sci Part A: Polym Chem 2011, 49, 1183.
29. Liu, D.; Chen, H.; Yin, P.; Ji, N.; Zong, G.; Qu, R. J Polym Sci Part A: Polym Chem 2011, 49, 2916.
30. Detrembleur, C.; Debuigne, A.; Jerome, C.; Phan, T. N. T.; Bertin, D.; Gigmes, D. Macromolecules 2010, 42, 8604.
31. Liu, X.-H.; Li, Y.-G.; Lin, Y.; Li, Y.-S. J Polym Sci Part A: Polym Chem 2007, 45, 1272.
32. Liu, X.-H.; Zhang, G.-B.; Lu, X.-F.; Liu, J.-Y. U.; Pan, D.; Li, Y.-S. J Polym Sci Part A: Polym Chem 2006, 44, 490.
33. Debuigne, A.; Michaux, C.; Jérôme, C.; Jérôme, R.; Poli, R.; Detrembleur, C. Chem—Eur J 2008, 14, 7623.
34. Nicolas, J.; Brusseau, S.; Charleux, B. J Polym Sci Part A: Polym Chem 2010, 48, 34.
35. Stewart, M. E.; George, S. E.; Miller, R. L.; Paul, D. R. Polym Eng Sci 1993, 33, 675.
36. Lessard, B.; Maric, M. Macromolecules 2008, 41, 7870.
37. Asua, J. M.; Beuermann, S.; Buback, M.; Castignolles, P.; Charleux, B.; Gilbert, R. G.; Hutchinson, R. A.; Leiza, J. R.; Nikitin, A. N.; Vairon, J.-P.; Herk, A. M. V. Macromol Chem Phys 2004, 205, 2151.
38. Hutchinson, R. A.; Beuermann, S.; Paquet, D. A.; McMinn, J. H.; Jackson, C. Macromolecules 1998, 31, 1542.
39. Gruendling, T.; Junkers, T.; Guilhaus, M.; Barner-Kowollik, C. Macromol Chem Phys 2010, 211, 520.
40. Azuma, C.; Dias, M. L.; Mano, E. B. Makromol Chem Macromol Symp 1986, 2, 169.
41. Reddy, G. R.; Kalpagam, V. J Polym Sci Part B: Polym Phys 1976, 14, 759.
42. Shimura, Y. J Polym Sci Part A-2: Polym Phys 1966, 4, 423.
43. Kössler, I.; Neptopilik, M.; Schulz, G.; Gnauk, R. Polym Bull 1982, 7, 597.
44. Lessard, B.; Graffe, A.; Maric, M. Macromolecules 2007, 40, 9284.
45. Lessard, B.; Tervo, C.; De Wahl, S.; Clerveaux, F. J.; Tang, K. K.; Yasmine, S.; Andjelic, S.; D'Alessandro, A.; Maric, M. Macromolecules 2010, 43, 868.
46. Junkers, T.; Koo, S. P. S.; Barner-Kowollik, C. Polym Chem 2010, 1, 438.
47. Buback, M.; Gilbert, R. G.; Hutchinson, R. A.; Klumperman, B.; Kuchta, F.-D.; Manders, B. G.; O'Driscoll, K. F.; Russell, G. T.; Schweer, J. Macromol Chem Phys 1995, 196, 3267.
48. Benoit, D.; Grimaldi, S.; Robin, S.; Finet, J. P.; Tordo, P.; Gnanou, Y. J Am Chem Soc 2000, 122, 5929.
49. Fukuda, T.; Ma, Y.-D.; Inagaki, H. Macromolecules 1985, 18, 17.
50. Fischer, H. J Polym Sci Part A: Polym Chem 1999, 37, 1885.
51. Charleux, B.; Nicolas, J.; Guerret, O. Macromolecules 2005, 38, 5485.
52. Ma, Y.-D.; Sung, K.-S.; Tsujii, Y.; Fukuda, T. Macromolecules 2001, 34, 4749.
53. Beuermann, S.; Buback, M. Prog Polym Sci 2002, 27, 191.
54. Keramopoulos, A.; Kiparissides, C. Macromolecules 2002, 35, 4155.
55. Hill, D. J. T.; O'Donnell, J. H.; O'sullivan, P. W. Macromolecules 1982, 15, 960.
56. Dire, C.; Charleux, B.; Magnet, S.; Couvreur, L. Macromolecules 2007, 40, 1897.
57. Roberts, G. E.; Davis, T. P.; Heuts, J. P. A.; Ball, G. E. Macromolecules 2002, 35, 9954.
58. Mayo, F. R.; Lewis, F. M. J Am Chem Soc 1944, 66, 1594.
59. Fineman, M.; Ross, S. D. J Polym Sci 1950, 5, 259.
60. Kennedy, J. P.; Kelen, T.; Tudos, F. J Polym Sci Part A: Polym Chem 1975, 13, 2277.
61. Kelen, T.; Tüdos, F. J Macromol Sci Chem 1975, 9, 1.
62. Dube, M.; Sanayei, R. A.; Penlidis, A.; O'Driscoll, K. F.; Reilly, P. M. J Polym Sci Part B: Polym Chem 1991, 29, 703.
63. Kazemi, N.; Duever, T. A.; Penlidis, A. Macromol React Eng 2011, 5, 383.
64. Meyer, V. E.; Lowry, G. G. J Polym Sci Part A: Polym Chem 1965, 3, 2843.
65. Bag, D. S.; Maiti, S. J Polym Sci Part B: Polym Phys 1997, 35, 2049.
66. Tidwell, P. A.; Mortimer, G. A. J Polym Sci Part A: Gen Pap 1965, 3, 369.
67. Burke, A. L.; Duever, T. A.; Penlidis, A. J Polym Sci Part A: Polym Chem 1993, 31, 3065.
68. Greenley, R. Z. In Polymer Handbook, 4th ed.; Brandup, J., Immergut, E. H., Grulke, E. A., Eds.; Wiley: New York, 1999; Section III, Table I, p 309.
69. Tang, C.; Kowalewski, T.; Matyjaszewski, K. Macromolecules 2003, 36, 1465.
70. Hamielec, A. E.; Tobita, H. In Ullman's Encyclopedia of Industrial Chemistry, 5th ed.; VCH: Weinheim, DE, 1992; Vol. A21, p 305.
71. Khesareh, R.; McManus, N. T.; Penlidis, A. J Appl Polym Sci 2006, 100, 843.
72. Garcia-Rubio, L. H.; Hamielec, A. E. J Appl Polym Sci 1979, 23, 1397.
73. Nair, A. S.; Muthana, M. S. Makromol Chem 1961, 47, 138.
74. Kapur, G. S.; Brar, A. S. Makromol Chem 1991, 192, 2733.
75. Greenley, R. Z. J Macromol Sci Chem 1975, 9, 1.
76. El-Sabee, M. Z.; Ahmed, A. H.; Mawaziny, S. Eur Polym J 1974, 10, 1149.